Increased Facilitatory Connectivity from the Pre-SMA to the Left Dorsal Premotor Cortex during Pseudoword Repetition

Gesa Hartwigsen[1,2,3], Dorothee Saur[3], Cathy J. Price[4], Annette Baumgaertner[1,2,5], Stephan Ulmer[6,7], and Hartwig R. Siebner[1,2,8]

Abstract

■ Previous studies have demonstrated that the repetition of pseudowords engages a network of premotor areas for articulatory planning and articulation. However, it remains unclear how these premotor areas interact and drive one another during speech production. We used fMRI with dynamic causal modeling to investigate effective connectivity between premotor areas during overt repetition of words and pseudowords presented in both the auditory and visual modalities. Regions involved in phonological aspects of language production were identified as those where regional increases in the BOLD signal were common to repetition in both modalities. We thus obtained three seed regions: the bilateral pre-SMA, left dorsal premotor cortex (PMd), and left ventral premotor cortex that were used to test 63 different models of effective connectivity in the premotor network for pseudoword relative to word repetition. The optimal model was identified with Bayesian model selection and reflected a network with driving input to pre-SMA and an increase in facilitatory drive from pre-SMA to PMd during repetition of pseudowords. The task-specific increase in effective connectivity from pre-SMA to left PMd suggests that the pre-SMA plays a supervisory role in the generation and subsequent sequencing of motor plans. Diffusion tensor imaging-based fiber tracking in another group of healthy volunteers showed that the functional connection between both regions is underpinned by a direct cortico-cortical anatomical connection. ■

INTRODUCTION

Recent functional anatomic models of language processing proposed that the repetition of pseudowords (i.e., pronounceable nonwords) activates a neural network mapping auditory input onto motor articulatory representations (Hickok & Poeppel, 2004). Frontal premotor regions, in particular, have been associated with articulatory planning and initiation of speech (Sörös et al., 2006; Shuster & Lemieux, 2005).

Among these regions, the pre-SMA has been assigned a key role in the repetition of speech stimuli. The pre-SMA was consistently activated during the repetition of pseudowords or phonemes in a variety of previous functional imaging studies in healthy volunteers (Papoutsi et al., 2009; Rauschecker, Pringle, & Watkins, 2008; Burton, Noll, & Small, 2001). Some studies demonstrated an involvement of the pre-SMA in the repetition of pseudowords with increasing complexity (i.e., the encoding of an abstract sequence into a motor plan; Peeva et al., 2010; Alario, Chainay, Lehericy, & Cohen, 2006; Bohland & Guenther, 2006). Because the pre-SMA is a key area for the preparation of speech and the initiation of vocal tract movements, this region has been labeled as the "starting mechanism of speech" (Ackermann & Ziegler, 2010; Botez & Barbeau, 1971). Finally, lesions in the (pre-)SMA have been associated with deficits in the sequencing of speech plans and speech initiation (Alm, 2004; Ziegler, Kilian, & Deger, 1997).

Other non-speech motor control studies have further demonstrated that the pre-SMA is involved in the motor control of sequential movements (Tanji & Hoshi, 2001; Halsband, Ito, Tanji, & Freund, 1993). It has therefore been suggested that the pre-SMA contributes to internal monitoring and preparatory activation of the temporal sequence of behavioural events (Shima & Tanji, 2000).

In addition to the pre-SMA, lateral premotor areas have also been implicated in pseudoword or phoneme production in previous studies (Peeva et al., 2010; Saur et al., 2008; Alario et al., 2006; Bohland & Guenther, 2006; Guenther, Ghosh, & Tourville, 2006). Some studies reported activation of the dorsal premotor cortex (PMd)

[1]Christian-Albrechts-University, Kiel, Germany, [2]NeuroImage-Nord, Hamburg-Kiel-Lübeck, Germany, [3]University of Leipzig, [4]University College London, [5]Fresenius University of Applied Sciences, Hamburg, Germany, [6]University Hospital of Schleswig-Holstein, Kiel, Germany, [7]University Hospital Basel, [8]Copenhagen University Hospital Hvidovre

during pseudoword repetition or reading (Saur et al., 2008; Mechelli et al., 2005), whereas other studies found activation of the ventral premotor cortex (PMv) and adjacent posterior inferior frontal gyrus during phoneme or syllable production (Alario et al., 2006; Bohland & Guenther, 2006; Guenther et al., 2006). Both regions are assumed to be part of to the motor speech network that maps sounds onto articulation during stimulus repetition (Hickok, Houde, & Rong, 2011).

Although the pre-SMA as well as lateral premotor areas have been implicated in articulatory preparation and initiation of speech, none of the above-mentioned studies provide any insights into the connectivity and information flow within this network. Consequently, it remains unclear how the premotor areas interact and drive one another during pseudoword repetition.

Here we used fMRI with dynamic causal modeling (DCM; Friston, Harrison, & Penny, 2003) to investigate how pseudoword repetition influences the regional interactions within the premotor network for pseudoword repetition, which comprises pre-SMA, PMd, and PMv. DCM has been used in a variety of previous studies to investigate different aspects of language processing (den Ouden et al., 2012; Richardson, Seghier, Leff, Thomas, & Price, 2011; Seghier, Josse, Leff, & Price, 2011; Leff et al., 2008; Mechelli et al., 2005). However, there have been no investigations of regional interactions during pseudoword repetition.

On the basis of the speech repetition studies cited above, we expected that an increased task-related activation of the pre-SMA during pseudoword repetition would reflect the planning or initiation of speech movements.

Our first aim was to identify the most likely source of the driving input to the premotor network for pseudoword repetition. We thus compared a variety of alternative network architectures testing all possible combinations of driving inputs among the three premotor regions. If the pre-SMA can indeed be labeled as the starting mechanism of speech, then we would expect that the best fit of the driving input would be into pre-SMA.

Because of the key role of the pre-SMA in speech repetition described above, we further expected an increased functional influence of the pre-SMA on lateral premotor areas engaged in the preparation of the final output during pseudoword repetition. Third, we were also interested in identifying whether the assumed influence of the pre-SMA was inhibitory or facilitatory. A facilitatory influence would be compatible with the notion of the pre-SMA as a key node for the encoding of sequences into motor plans. On the other hand, pre-SMA activation has also been associated with the inhibition of speech responses during pseudoword reading (Xue, Aron, & Poldrack, 2008). An inhibitory influence of the pre-SMA might thus explain the previously reported stronger activation of this area during unfamiliar speech versus familiar speech (i.e., the repetition of pseudowords relative to words; Alario et al., 2006) and during volitional relative to stimulus-driven speech (Tremblay & Gracco, 2006) because unfamiliar speech might require the inhibition of more prepotent responses (i.e., from associated words that are similar to but different from the target stimulus) whereas volitional speech might require the inhibition of inappropriate speech.

Finally, diffusion tensor imaging (DTI)-based tractography allowed us to assess whether effective connectivity might be mediated via a direct cortico-cortical connection.

METHODS

Participants

Seventeen right-handed native German speakers (10 women, ages 21–30 years, mean = 23.8 years, *SD* = 2.2 years) with no history of neurological disorders or head injury participated in the fMRI experiment. Seventeen different right-handed healthy native German speakers (10 women, ages 20–29 years, mean = 22.5 years, *SD* = 2.7 years) were included in the DTI experiment. Written informed consent was obtained from all participants before the experiment. Handedness was tested with the German version of the Edinburgh Handedness Inventory (Oldfield, 1971). The study was performed according to the guidelines of the Declaration of Helsinki and approved by the Ethics Committees of the Medical Faculty of the Universities of Kiel (fMRI experiments) and Leipzig (DTI experiments).

Experimental Design and Tasks

The fMRI study used a 2 (Task: repetition of pseudowords vs. words) × 2 (Modality: auditory vs. visual stimuli) factorial event-related within-subject design (Figure 1). This design resulted in four event types: auditory words (AW), visual words (VW), auditory pseudowords (APW), and visual pseudowords (VPW). The same 60 stimuli (30 pseudowords and words each) were presented auditorily and visually to minimize stimulus-induced differences in the planned comparisons between modalities (Devlin, Matthews, & Rushworth, 2003).

Before scanning, participants had a training session outside the scanner during which both tasks were practiced and all experimental stimuli were presented to reduce the novelty of the pseudoword relative to the word stimuli. Participants were trained to move their head as little as possible when repeating the stimuli, and the head was fixated in the head coil using foam cushions. The experiment started with a written instruction to repeat the written or spoken stimulus as soon as it was finished (auditory stimuli) or vanished from the screen (visual stimuli). Experimental stimuli were divided into two runs with 10 blocks each (Figure 1A), resulting in five blocks for each of the four conditions (i.e., AW, VW, APW, VPW). Each run started and ended with a rest block. Block duration was set to 36 sec, and blocks were separated by 16-sec rest, leading to a total duration of approximately 9 min per run.

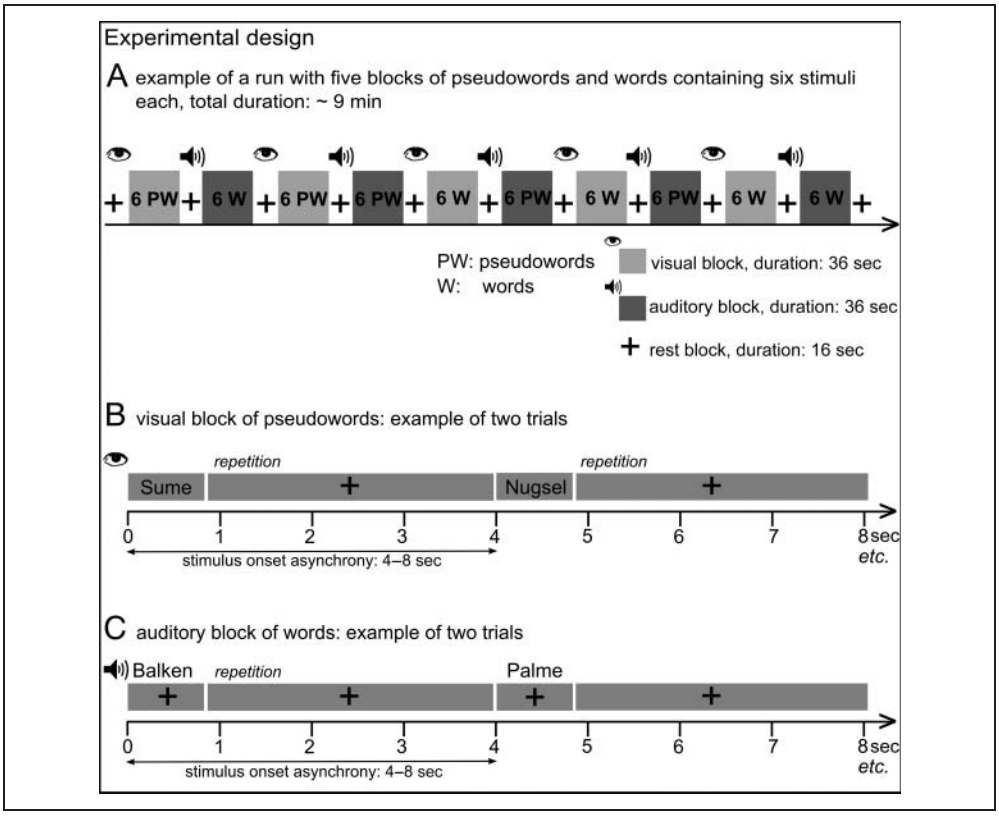

Figure 1. Experimental design. (A) Example of a run. The experiment consisted of two runs with five blocks of pseudowords and words each. The order of runs was randomized across participants. At the end of each rest block, a visual cue indicated whether the next block would consist of auditorily or visually presented pseudowords or words, respectively. The onset of the cue was jittered such that it appeared 9.5–12.5 sec after the rest block had started. (B) Visual block of pseudowords. Example of two trials. Each block consisted of six pseudowords (or words) with a mean duration of 0.83 sec that were separated by a randomly set SOA of 4–8 sec. (C) Auditory block of words. Each block consisted of six pseudowords (or words) that were separated by a randomly set SOA of 4–8 sec.

During rest blocks, a fixation cross was presented. At the end of each rest period, a visual nonverbal cue indicated the following block. Cues consisted of a symbol of either an eye (indicating that the next block would contain visually presented stimuli) or a loudspeaker (indicating that the next block would contain auditorily presented stimuli) in a red or blue box. Blue boxes indicated that the next block would contain pseudowords; red boxes indicated real word presentation. Stimulus type (pseudowords or words) and modality (auditory or visual stimulus presentation) were held constant during each block to ensure a constant cognitive set.

Cue onset was jittered such that the cue appeared 9.5–12.5 sec after the rest block onset and remained on the screen for 2.5 sec. Thereafter, a fixation cross appeared, which remained on screen until the first stimulus of the following task block was presented (visual stimuli; Figure 1B) or during the whole following task block for auditory stimuli (Figure 1C). After stimulus presentation, subjects overtly repeated the respective stimulus.

Each block contained six pseudowords or words that were separated by a randomly assigned SOA of between 4 and 8 sec. In visual blocks, a fixation cross again appeared after stimulus presentation. The duration of stimulus presentation for visually presented stimuli was matched to the mean duration of auditory stimuli. The order of runs, stimulus blocks, and presentation modalities was pseudorandomized across subjects such that no more than one block within the same stimulation modality was presented consecutively.

This study served as control condition for a larger investigation applying TMS to different frontal areas for pseudoword repetition (Hartwigsen et al., unpublished data). We thus applied an ineffective "sham" stimulation over the posterior inferior frontal gyrus before the fMRI sessions (i.e., offline). This was established by placing one TMS coil over the target area and a second coil in an angle of 90° over the first coil. Only the second coil was connected to the stimulator and charged without effectively stimulating the brain (see Hartwigsen et al., 2010, for a similar sham procedure). Because task processing and sham TMS were separated in time and the stimulation coil did not directly touch the head, we are confident that our TMS procedure did not influence task processing or neuronal activity here.

After scanning, participants quickly indicated on a questionnaire which of the pseudowords used in the experiment had been familiar to them or had reminded them of an existing word. This allowed us to model the pseudowords associated with existing words as a separate regressor and thus ensured that the pseudowords included did not have any associated meaning.

Stimuli

Thirty two-syllable German nouns representing concrete items were used for stimulus presentation. Only highly frequent, unambiguous nouns from the CELEX lexical database for German (Centre for Lexical Information, Max Planck Institute for Psycholinguistics, The Netherlands)

were selected. All words were stressed on their first syllable and were controlled for their phoneme structure. One third of the items had a CVCV structure (e.g., "Dose" [*English: "box"*]), one-third had a CVCCV structure (e.g., "Palme" [*English: "palm tree"*]), and the remaining one-third had a CVCCVC structure (e.g., "Balken" [*English: "arbor"*]).

Thirty pseudowords were constructed with the aid of WordGen 1.0. (Duyck, Desmet, Verbeke, & Brysbaert, 2004; users.ugent.be/~wduyck/wwgman.htm) by dividing the syllables of the real words and rearranging them to meaningless nonwords that were matched for bigram frequency according to Dollaghan and Campbell (1998). The list of pseudowords was matched to the real word list such that all items were stressed on their first syllable and had a comparable phoneme structure (i.e., one-third had a CVCV structure ["Sume"], one-third had a CVCCV structure ["Belse"], and one-third had a CVCCVC structure ["Nugsel"]) and a comparable stimulus length. Auditory versions of the stimuli were recorded by a professional female speaker and had an average duration of 0.85 sec. Finally, the intensity threshold was set to 80 dB for all auditory stimuli using Praat software (www.praat.org/).

Stimulus Presentation and Response Collection

For auditory stimulus presentation and overt response recording, we used MR-compatible electrodynamic headphones (HP-SC01) with a passive built-in dual-channel microphone (MIC-DCHS-02; MR ConFon GmbH, Magdeburg, Germany, www.mr-confon.de). Speech responses were recorded with OptiMRI software, which automatically preprocesses the dual-channel recordings by reducing the whole frequency spectrum of the scanner noise by 20 dB in relation to the speech signal. To optimize speech signals, postprocessing of the speech responses additionally included the application of an automatic notch filter (50–60 Hz). This procedure ensured that the recorded vocal responses were of high quality and could easily be identified as correct or incorrect. Individual speech onsets and durations were measured with Audacity software Version 1.3 (audacity.sourceforge.net/).

Presentation of stimuli and task sequence were controlled using E-PRIME (Psychology Software Tools, Inc., Pittsburgh, PA; Version 1.1) implemented in IFIS-SA system software (www.invivocorp.com/fmri/ifis.php; Version 1.1).

fMRI

Functional imaging was performed on a Philips 3-T scanner (Philips, Best, the Netherlands), using a gradient EPI sequence (repetition time [TR]/echo time [TE] = 2500/35 msec, flip angle = 90°, matrix = 64 × 64 pixel, voxel size = 3.38 × 3.38 × 3 mm^3) with BOLD contrast for the acquisition of T2*-weighted images. A total of 214 volumes consisting of 38 slices was acquired continuously during each run. Additionally, T1-weighted anatomical images were acquired with an MPRAGE sequence in sagittal orientation (voxel size = 1 × 1 × 1 mm^3, TR = 1.3 sec, TE = 3.78 msec). DTI data were collected on a Siemens Verio 3-T scanner (Siemens, Erlangen, Germany). We acquired axial whole-brain diffusion-weighted images with a double-spin echo sequence (60 directions; b = 1000 sec/mm^2, 88 slices, voxel size = 1.7 × 1.7 × 1.7 mm, no gap, TR = 12.9 sec, TE = 100 msec, field of view = 220 × 220 mm^2) plus seven volumes without diffusion weighting (b = 0 sec/mm^2) at the beginning of the sequence and after each block of 10 diffusion weighted images. For post-processing, a second T1-weighted anatomical scan was acquired with an MPRAGE sequence in sagittal orientation (voxel size = 1 × 1 × 1.5 mm^3, TR = 1.3 sec, TE = 3.46 msec).

Statistical Analyses

fMRI Data

Task-related changes in the BOLD signal were analyzed using Statistical Parametric Mapping (SPM 5/8, Wellcome Trust Centre for Neuroimaging, www.fil.ion.ucl.ac.uk/spm/) implemented in Matlab 7.7 (The Mathworks, Inc., Natick, MA; Friston, Ashburner, et al., 1995). During preprocessing, all functional EPI images were corrected for different acquisition times of signals by shifting the signal measured in each slice relative to the acquisition of the middle slice. All volumes were then realigned and unwarped to account for motion-induced artifacts (Andersson, Hutton, Ashburner, Turner, & Friston, 2001). We chose the unwarping procedure because it has been argued that there may be residual movement-related variance present in fMRI time series even after realignment that causes loss of sensitivity and, potentially, also specificity. Therefore, it has been suggested that the "unwarping tool" may be a valid alternative that significantly reduces movement-related variance (Andersson et al., 2001).

The individual T1-weighted image was coregistered to the mean functional EPI image and segmented using the standard tissue probability maps provided in SPM5 with a medium bias regularization. The resulting segmentation information was used for a second segmentation of the individual T1 image without any bias regularization. Afterwards, the resulting image was normalized and resampled to 1 × 1 × 1 mm^3 voxels. The functional EPI images were then normalized to this T1 image and resampled to 3 × 3 × 3 mm^3 voxels. Finally, all normalized images were smoothed with an isotropic 8-mm FWHM Gaussian kernel to account for intersubject anatomical differences and allow valid statistical inference according to Gaussian random field theory (Friston, Holmes, et al., 1995).

Statistical analyses of the functional images were performed in two steps. At the first level, the two runs were modeled separately, each consisting of at least five regressors including the four different experimental conditions

(i.e., AW, VW, APW, and VPW) and a regressor modeling the onset of the instructions. If appropriate, two additional regressors for incorrectly repeated stimuli or pseudowords judged as real words were included. Although Task and Modality were blocked, each trial was modeled separately, in an event-related analysis, allowing us to precisely model error trials without discarding the whole respective block. All of the onsets in each regressor were convolved with a canonical hemodynamic response function as implemented in SPM5. To ensure that the regressors were sampled in the middle point, microtime resolution was specified equally to the number of slices (i.e., 38) and microtime onset was specified equally to the reference middle slice (i.e., 19). This procedure ensures that the middle slice (in time) is never more than TR/2 away from any other slice, although it is nearly twice that TR away from the last slice if one sets the microtime onset to the first slice (SPM mailing list: https://www.jiscmail.ac.uk/cgi-bin/webadmin?A2=SPM;70bf5c7f.0904).

Voxel-wise regression coefficients for all conditions were estimated using the least squares method within SPM5, and statistical parametric maps of the t statistic (SPM{t}) were generated from each condition.

The data for the second stage of analysis comprised pooled parameter estimates for each of these contrasts across all participants and both runs in a random-effects analysis using a flexible factorial within-subject ANOVA design including a correction for nonsphericity.

We used the Restricted Maximum Likelihood method in the SPM8 design specification for sphericity correction at the second-level inference (Friston, Stephan, Lund, Morcom, & Kiebel, 2005).

The specification of Task (pseudoword vs. word repetition) and Modality (auditory vs. visual stimulus presentation) resulted in a 2 × 2 condition matrix for each subject. T-contrasts were computed for the main effect of each condition. We also computed conjunction analyses to delineate areas being activated across both visually and auditorily presented pseudowords and words and for pseudoword in contrast to real word repetition. We thus applied conjunction analyses under the conservative conjunction null hypothesis (Nichols, Brett, Andersson, Wager, & Poline, 2005). Main effects and conjunctions of main effects were thresholded at $p < .05$, corrected for multiple comparisons across the whole brain using the conservative family-wise error (FWE) method. For the differential effects directly contrasting pseudoword with word repetition, we used an initial height threshold of $p < .001$, uncorrected for the whole brain. Note that, for the modality-independent conjunction, the initial threshold had to be bottomed to $p < .01$ to obtain significant activation in the lateral premotor areas. We then applied small volume corrections (SVC) at a significance level of $p < .05$, FWE-corrected, to our a priori ROIs in the pre-SMA, PMd, and PMv. For each SVC, we defined a spherical ROI with a diameter of 10 mm. The center of the pre-SMA ROI was based on the mean coordinates across two recent studies (Xue et al., 2008; Alario et al., 2006) that reported activation for pseudoword repetition (and reading) in the pre-SMA ($x = 8$, $y = 15$, $z = 58$; Montreal Neurological Institute [MNI]). Accordingly, the centers of a SVC in left PMd ($x = -48$, $y = 0$, $z = 36$; MNI) and left PMv ($x = -57$, $y = 15$, $z = 5$; MNI) were taken from two different speech production studies reporting increased activity in two distinct areas of the lateral premotor cortex during either pseudoword repetition (PMd: Saur et al., 2008) or simulated syllable production (PMv: Guenther et al., 2006).

The SPM anatomy toolbox (Version 1.6; Eickhoff et al., 2005) and the WFU PickAtlas Tool (Version 2.4 Wake Forest University of School of Medicine) were used for anatomical localization of activation peaks (Figures 2 and 3).

DCM

Effective connectivity in the premotor network for pseudoword repetition was tested with DCM 10 (Stephan et al.,

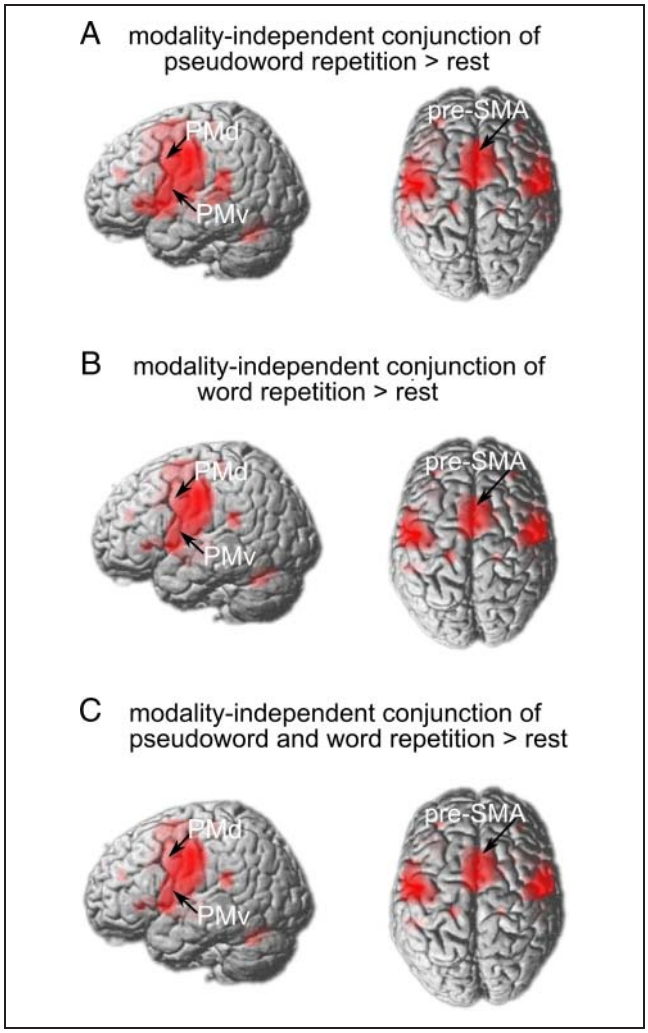

Figure 2. Modality independent conjunctions for the main effects of (A) pseudoword repetition, (B) word repetition, and (C) pseudoword and word repetition ($p < .05$ FWE-corrected).

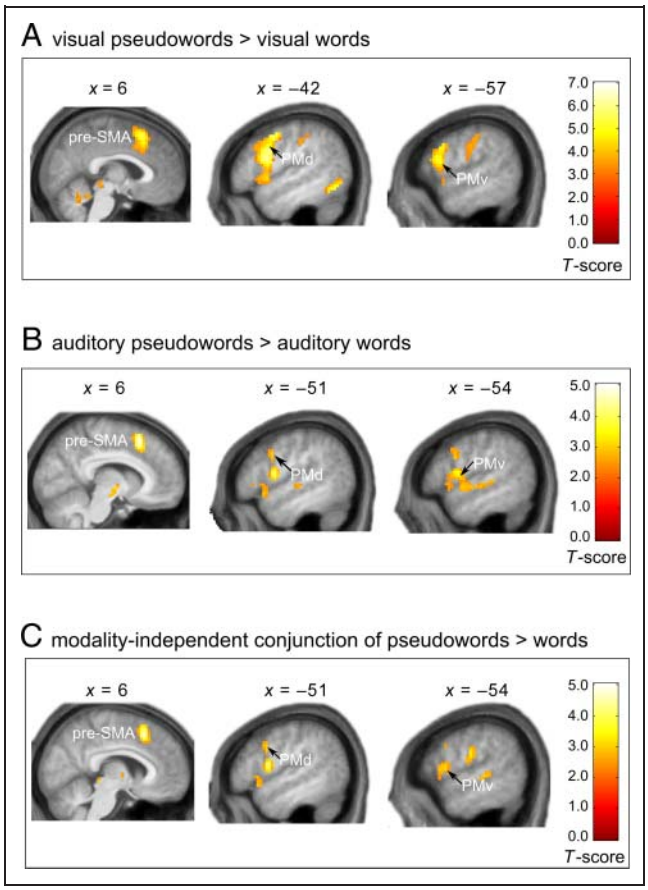

Figure 3. Differential effects of pseudoword > word repetition. All panels display significant activation clusters within our three premotor ROIs (from left to right: pre-SMA, PMd, PMv). (A) Comparison of visually presented pseudowords > words. (B) Comparison of auditorily presented pseudowords > words. (C) Conjunction across auditory and visual modalities for pseudoword > word repetition. All comparisons were thresholded at $p < .001$ uncorrected (modality-independent conjunction, $p < .01$ uncorrected) and corrected for multiple comparisons using SVCs ($p < .05$, FWE-corrected). Spatial references are given in MNI space.

2010) in SPM8. DCM allows for an investigation of the interaction of a predefined set of brain regions during different experimental contexts (Friston et al., 2003). The strength and the direction of regional interactions are computed by comparing the observed regional BOLD responses with the BOLD responses that are predicted by a neurobiologically plausible model. The model describes how activity in and interactions among regional neuronal populations are modulated by external inputs (i.e., the experimental task conditions) and how the ensuing neuronal dynamics translate into the measured BOLD signal (Leff et al., 2008). The model parameters are adjusted with an iterative Bayesian estimation, such that a free energy bound on the model evidence is optimized. As a result, three types of parameters are calculated: the direct influences of the external input or stimuli on regional activity (i.e., the driving input), the strength of the intrinsic connections between two regions in the absence of modulating experimental effects, and the changes in the intrinsic connectivity between regions induced by the experimental design (i.e., the modulatory effects of pseudoword vs. word repetition; Mechelli et al., 2005).

The aim of our DCM analysis was to (1) identify the most likely source of the driving input in the premotor network for pseudoword repetition, (2) identify the connections modulated by pseudoword repetition, and (3) identify whether this modulation was facilitatory or inhibitory.

The model space thus included 63 different models with full intrinsic connectivity (Figure 4). The driving input was set to either of the three premotor ROIs alone and to all possible combinations between these regions (Figure 4A) and the modulatory effects of two task conditions (pseudoword vs. word repetition) on the connections between these regions were specified for each subject (Figure 4B). The seed areas for the three premotor regions were derived from the modality-independent conjunction of pseudoword repetition and word repetition versus rest individually for each subject (mean coordinates for pre-SMA across subjects: $x, y, z = 5, 13, 57$; PMd: $x, y, z = -51, 0, 36$; PMv: $x, y, z = -57, 13, 5$; all ps $< .05$ FWE-corrected; Table 2).

First, the DCM models were specified for each subject. This required the specification of a new design matrix at the individual level, modeling the conditions of interest for the DCM analysis (i.e., one regressor modeling both correctly and incorrectly repeated pseudoword and word onsets across auditorily and visually presented stimuli, one regressor including only correct word onsets and one regressor including only correct pseudoword onsets). Subsequently, the first eigenvariate of the fMRI signal for our three seed regions was extracted at the individual level at a liberal threshold of $p < .001$ uncorrected (Friston et al., 1997) within a sphere of 10 mm around the mean group coordinate derived from the modality-independent conjunction of pseudoword and word repetition versus rest (see above) separately for each run. These data were included in the model specification for our DCMs.

For model selection across participants, we used a random-effects Bayesian model selection procedure (Stephan et al., 2010) to identify the most likely among our 63 candidate models given the observed fMRI data. To this end, all models are tested against each other. The models' probabilities are estimated, and inference is based on exceedance probabilities, reflecting the probability that this model is a better fit to the data than any other model of those tested.

Finally, subject-specific estimates for the nine parameters of interest in the winning model (i.e., the driving input, the strength of the intrinsic connections between the three premotor sites, and the impact of the modulation on the relevant connections by pseudoword or word repetition) were entered into Bonferroni-corrected two-sided one-sample t tests to test differences from zero.

Additionally, a paired t test was used to test whether the modulation was stronger for pseudoword compared with word repetition.

We additionally performed a family-level inference based on model space partitioning (Stephan et al., 2010) to identify the most likely winning family. In a family analysis, models are grouped according to the presence of one or more features that are shared by that subset of models (e.g., the same driving input). The family with the highest exceedance probability value again represents the model group that is most plausible given the data (Stephan et al., 2010).

Probabilistic DTI-based Fiber Tracking

The aim of fiber tracking was to identify the anatomical connection mediating the effective connectivity between the pre-SMA and PMd (or PMv) as revealed by our DCM analysis (Figures 5 and 6). Fiber tracking was based on a recently developed pathway extraction (Kreher et al., 2008) using the DTI and Fiber Toolbox (www.uniklinik-freiburg.de/mr/live/arbeitsgruppen/diffusion_en.html) implemented in SPM8. First, the diffusion tensor was computed (Basser, Mattiello, & LeBihan, 1994). A Monte Carlo simulation of random walks was then used to calculate probabilistic maps separately for our seed regions in the pre-SMA (fMRI seed: $x = -6$, $y = 12$, $z = 57$), PMd (fMRI seed: $x = -51, y = 0, z = 36$), and PMv (fMRI seed: $x = -57$, $y = 13$, $z = 5$). Note that, for the pre-SMA, we used a subpeak coordinate in the left hemisphere within the large bilateral pre-SMA cluster as seed region because we were interested in delineating the left hemispheric connectivity profile between the premotor regions. In all seed maps, the obtained visiting frequency of a voxel reflects the degree of connectivity to the seed region. To identify the most probable region-to-region connections between left pre-SMA and PMd or left pre-SMA and PMv, the probability maps for the respective seed regions were multiplied using the algorithm of Kreher et al. (2008). This method allows for the extraction of the most probable direct pathway between two seed regions without using a priori knowledge about the presumed course. The resulting values represent a voxel-wise estimation of the probability index that a voxel is part of the connecting fiber bundle of interest (PIBI). The combined map was scaled to the range between 0 and 1 and spatially normalized into the standard MNI. Group maps were computed by averaging the combined maps from all subjects. Following Saur et al. (2008), a conservative PIBI value of >0.0148 was chosen to remove random artifacts, which excluded 95% of the voxels with PIBI > 10^{-6}.

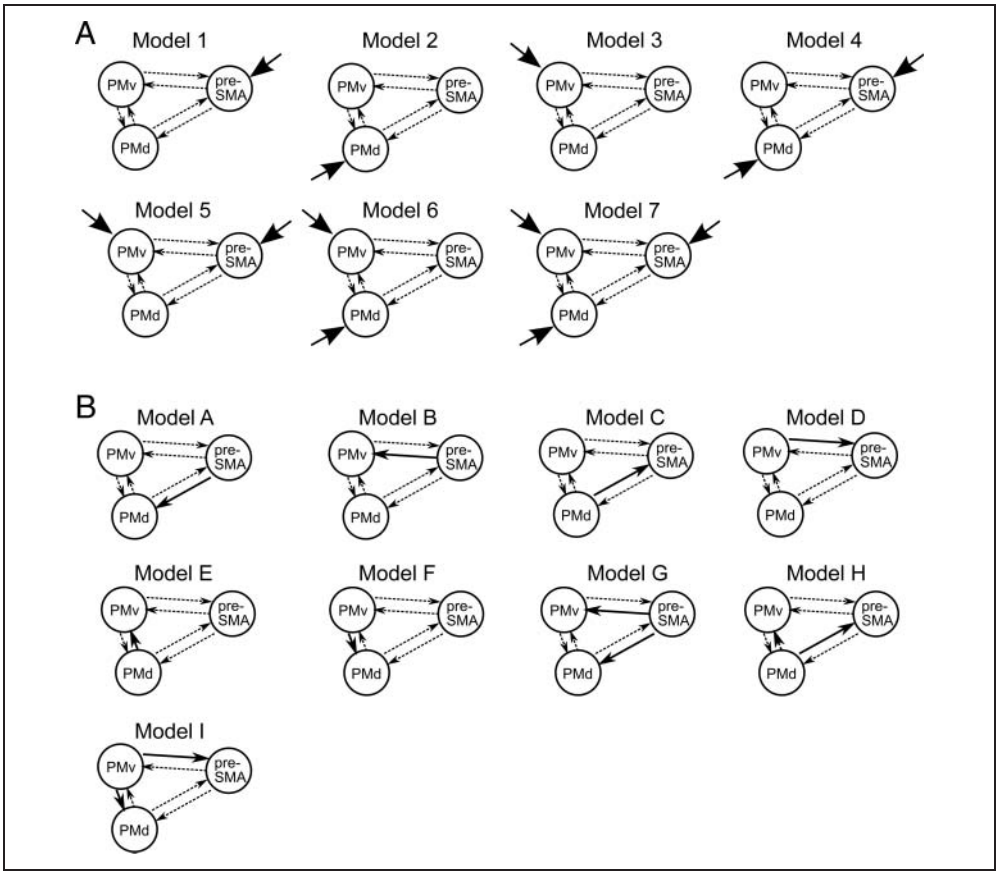

Figure 4. Illustration of the different DCM models. (A) Seven models that differ with respect to the driving input regions (indicated by fat solid arrows). (B) Nine models with different external modulations by pseudoword versus word repetition (indicated by solid arrows between regions). The combination of both model types resulted in a total of 63 models. All models had the same intrinsic connections (shown as dotted arrows).

RESULTS

Behavioral Data

Participants' mean RTs (i.e., speech onset times), response durations, and error rates for all conditions are reported in Table 1. For each dependent measure, a two-way repeated-measures ANOVA was conducted using the factors Task (pseudoword vs. word repetition) and Modality (auditory vs. visual stimulus presentation). There were no significant main effects or interactions between the different conditions on either RTs (all $ps > .25$) or response durations (all $ps > .16$). Participants were overall very accurate. Errors comprised both omissions and wrong responses (e.g., "Nagsel" instead of "Nugsel"). Again, a repeated-measures ANOVA did not reveal any significant main effects or interactions between the different conditions (all $ps > .37$).

Imaging Data

Brain Regions Involved in Pseudoword and Word Repetition versus Rest

The modality-independent effects of pseudoword and word repetition versus rest were computed with conjunctions across stimulus modalities. The repetition of both stimulus types engaged a widespread bilateral temporofrontal network of pre- and postcentral regions previously associated with language production (Peeva et al., 2010; Bohland & Guenther, 2006; Price, 2000), including primary motor cortex, dorsal and ventral premotor areas, SMA, inferior frontal gyrus, superior and middle temporal gyrus, and the cerebellum (Figure 2 and Table 2). Overall, pseudowords and words activated the same regions. Of note, the pre-SMA, as well as PMd and PMv, were activated for both pseudoword repetition compared with rest and word repetition compared with rest (see Figure 2A, B and Table 2). These areas also showed strong activation increases when combined in a conjunction across auditorily and visually presented pseudowords and words (Figure 2C and Table 2). The modality-independent conjunction across auditorily and visually presented pseudowords and words was used to obtain peak coordinates for our premotor ROIs (i.e., pre-SMA: $x = 5, y = 13, z = 57$; PMd: $x = -51, y = 0, z = 36$; PMv: $x = -57, y = 13, z = 5$; all $ps < .05$; FWE-corrected) for the purpose of data extraction and subsequent DCM analyses (cf. DCM section). We note that the activation peaks for left PMd were located directly at the border between dorsal and

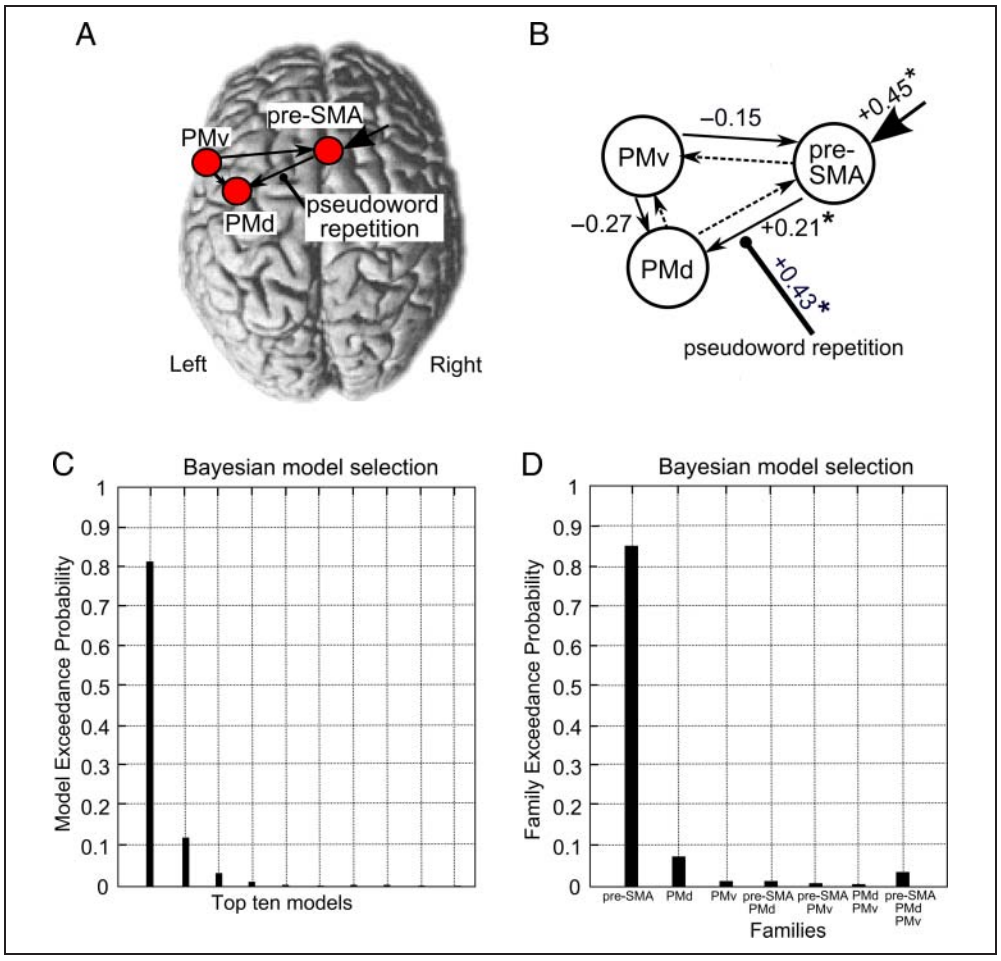

Figure 5. Results from the DCM analyses. (A) The winning model of the 63 tested models, with driving input to pre-SMA and modulation of the connection between pre-SMA and PMd by pseudoword repetition. (B) The mean parameter estimates for all significant intrinsic connections (shown as solid arrows), the driving input, and the modulation of the winning model. Connections that survived a Bonferroni correction for multiple comparisons are marked with an asterisk. (C) The model exceedance probabilities for the top 10 models compared with variational Bayesian model selection. Note that the exceedance probability does not exactly sum to 1 (or 100%) here as we only show the top 10 models for display reasons. The remaining 53 models contributed less than 1% each. (D) shows the model exceedance probabilities for each model of the family analysis. Family groups were divided according to the different driving inputs.

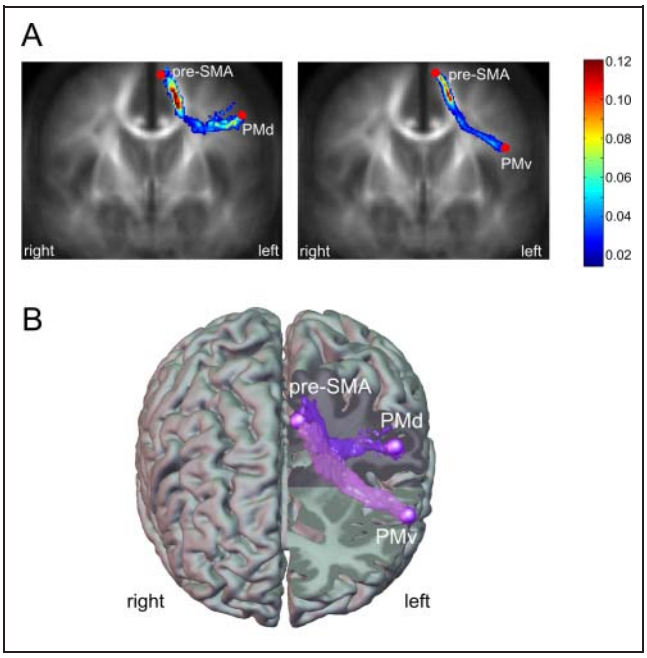

Figure 6. Fiber tract mediating functional connectivity in the premotor network for pseudoword repetition as revealed by probabilistic fiber tracking. (A) Mean maximum intensity projection map of 17 subjects visualized on the mean fractional anisotropy map (y range: −10:30; MNI space). The color coding represents the mean PIBI value (probability index forming part of the bundle of interest) across the group; the value at the top of the color bar represents the maximum mean PIBI value. (B) Three-dimensional tractography renderings illustrate the spatial orientation of the fiber network for pseudoword repetition. Seed spheres are visualized with a radius of 4 mm. PMd (fMRI seed: $x = -51, y = 0, z = 36$); PMv(fMRI seed: $x = -57, y = 13, z = 5$); pre-SMA (fMRI seed: $x = -6, y = 12, z = 57$).

PMv as defined by a previous meta-analysis (Mayka, Corcos, Leurgans, & Vaillancourt, 2006).

Brain Regions Involved in Pseudoword as Opposed to Word Repetition

We directly contrasted pseudoword repetition with word repetition to investigate whether our three premotor areas of interest would show stronger activation during pseudoword repetition. The bilateral pre-SMA showed strong activation for the unimodal comparisons of pseudoword versus word repetition for both visually presented stimuli ($x = 6, y = 18, z = 54$; $T = 4.61$; $p = .001$ FWE-corrected for multiple comparisons in the pre-SMA ROI; Figure 3A, left) and auditorily presented stimuli ($x = 6$, $y = 18$, $z = 48$; $T = 4.24$; $p = .001$ FWE-corrected in the pre-SMA ROI; Figure 3B, left). The modality-independent conjunction of pseudoword versus word repetition across auditorily and visually presented stimuli also showed strong activation of the bilateral pre-SMA ($x = 6$, $y = 18$, $z = 54$; $T = 3.92$; $p = .011$ FWE-corrected in the pre-SMA ROI; Figure 3C, left). Left PMd showed increased activation for the comparison of pseudoword versus word repetition in the visual modality ($x = -42$, $y = 0$, $z = 39$; $T = 5.55$; $p = .0001$ FWE-corrected in the PMd ROI; Figure 3A, middle). There were also trends toward increased activation in the auditory modality ($x = -51$, $y = 6$, $z = 36$; $T = 3.01$; $p = .071$ FWE-corrected in the PMd ROI; Figure 3B, middle) and for the modality-independent conjunction across auditorily and visually presented pseudowords versus words ($x = -51$, $y = 6$, $z = 37$; $T = 3.01$; $p = .071$ FWE-corrected in the PMd ROI; Figure 3C, middle). Finally, there was increased activity in left PMv for visually presented pseudowords versus words ($x = -57$, $y = 9$, $z = 9$; $T = 4.58$; $p = .001$ FWE-corrected in the PMd ROI; Figure 3A, right). There was also a trend toward increased activity in PMv for auditorily presented pseudowords versus words ($x = -54$, $y = 5$, $z = 0$; $T = 2.91$; $p = .096$ FWE-corrected in the PMv ROI; Figure 3B, right) and for the modality-independent conjunction across auditorily and visually presented pseudowords versus words ($x = -54$, $y = 6$, $z = 9$; $T = 2.91$; $p = .096$ FWE-corrected in the PMv ROI; Figure 3C, right).

Effective Connectivity in the Network for Pseudoword Repetition

Among the 63 models tested, variational Bayesian model selection identified Model 1 with driving input to

Table 1. Behavioral Results

Task	*RT ± SD (msec)*	*Response Duration ± SD (msec)*	*Error Rate ± SD (%)*
Pseudoword Repetition			
Auditory stimuli	920 ± 54	691 ± 96	0.015 ± 0.001
Visual stimuli	895 ± 38	689 ± 91	0.014 ± 0.001
Word Repetition			
Auditory stimuli	897 ± 47	695 ± 87	0.014 ± 0.001
Visual stimuli	887 ± 52	687 ± 89	0.014 ± 0.001

All measures are given in milliseconds (msec) or percentage of all trials.

Table 2. Areas for Pseudoword and Word Processing

Region	*Side*	*MNI Coordinates x y z (in mm)*			*T*	*Z*	*Cluster Size*
Modality-independent Conjunction of Auditory Pseudowords and Visual Pseudowords > Rest							
Primary motor cortex	L	−48	−12	36	25.86	Inf.	1997
Primary motor cortex	R	45	−12	36	23.89	Inf.	857
Pre-SMA	R	4	11	59	18.87	Inf.	627
Premotor cortex (dorsal part)	L	−48	0	36	16.21	Inf.	532
Premotor cortex (ventral part)	L	−54	15	5	13.54	Inf.	437
Cerebellum	R	15	−63	−21	13.09	Inf.	227
Cerebellum	L	−24	−66	−27	12.25	Inf.	215
Inferior frontal gyrus (pars opercularis)	L	−51	6	9	11.29	Inf.	231
Superior temporal gyrus	L	−48	−39	18	8.72	6.72	145
Primary motor cortex	L	−18	−30	60	8.11	6.40	33
Middle temporal gyrus	R	51	−30	0	7.52	6.09	103
Middle frontal gyrus	L	−30	42	24	6.68	5.59	30
Middle frontal gyrus	R	39	42	27	6.19	5.28	29
Modality-independent Conjunction of Auditory Words and Visual Words > Rest							
Primary motor cortex	L	−45	−12	39	24.45	Inf.	964
Primary motor cortex	R	48	−12	36	20.78	Inf.	817
Pre-SMA	R	5	13	57	13.57	Inf.	527
Premotor cortex (dorsal part)	L	−51	0	36	13.21	Inf.	302
Inferior frontal gyrus (pars opercularis)/premotor cortex (ventral part)	L	−54	9	9	13.47	Inf.	237
		−57	13	5	13.12	Inf.	
Cerebellum	R	15	−63	−21	12.78	Inf.	169
Cerebellum	L	−21	−60	−27	11.88	Inf.	134
Superior temporal gyrus	L	−48	−39	18	8.72	6.72	35
Primary motor cortex	L	−18	−30	60	8.11	6.40	34
Middle frontal gyrus	L	−30	42	24	6.46	5.45	28
Modality-independent Conjunction of Auditory Pseudowords and Visual Pseudowords and Auditory Words and Visual Words > Rest							
Primary motor cortex	L	−45	−12	39	24.45	Inf.	942
Primary motor cortex	R	48	−12	36	20.78	Inf.	691
Pre-SMA	**R**	**5**	**13**	**57**	**12.57**	**Inf.**	**481**
Premotor cortex (dorsal part)	**L**	**−51**	**0**	**36**	**12.71**	**Inf.**	**201**
Cerebellum	R	15	−63	−21	12.78	Inf.	168
Inferior frontal gyrus (pars opercularis)	**L**	−54	9	9	12.27	Inf.	**221**
PMv		**−57**	**13**	**5**	**11.21**	**Inf.**	
Cerebellum	L	−21	−60	−27	11.88	Inf.	127
Superior temporal gyrus	L	−48	−39	18	8.72	6.72	35
Primary motor cortex	L	−18	−30	60	8.11	6.40	28
Middle frontal gyrus	L	−30	42	24	6.46	5.45	28

All contrasts were thresholded at $p < .05$ FWE-corrected. Clusters represent local maxima. Selected ROIs for the DCM analysis are shown in **bold**. Inf. = Infinite (Z score > 8.0).

pre-SMA and modulation of the facilitatory connection from pre-SMA to PMd by pseudoword repetition as winning model across participants (Figure 5A). This model had an exceedance probability of 81% (Figure 5C) and a posterior model probability of 75%. Note that the second best model only reached an exceedance probability of 11%, and all other models were below 5%.

Figure 5B shows the winning model with the mean parameter estimates that are significantly different from zero. The only parameter values that survived a Bonferroni correction for multiple comparisons were the driving input to pre-SMA (mean estimate: +0.45; $p < .0001$), the intrinsic connection from pre-SMA to PMd (mean estimate: +0.21; $p < .001$), and the modulation of this connection by pseudoword repetition (mean estimate: +0.43; $p < .0001$; Table 3). This modulatory influence of pseudoword repetition on the connection between pre-SMA and PMd was facilitatory, corresponding to an increase in connectivity of about 156% relative to the intrinsic (positive) connection strength. Note that a direct comparison of the parameter estimates for pseudoword versus word repetition confirmed that the facilitatory effect was stronger for pseudowords than words (paired t test: $T = 5.16$; $p < .001$).

In line with the results from the conventional DCM analysis, the Bayesian comparison between the seven families of models with different driving inputs showed that those with driving input to pre-SMA generally better fitted the data, with a family exceedance probability of 85% (Figure 5D) and a posterior model probability of 78%.

Table 3. Mean Parameter Estimates for the Winning Model

Connection/Parameter	*Mean*	*SD*	*t*	*p*
Intrinsic Connections				
Pre-SMA → PMd	0.2139	0.2143	4.08	.001**
PMd → Pre-SMA	0.1379	0.2527	1.62	.071
Pre-SMA → PMv	0.1634	0.8765	1.35	.179
PMv → Pre-SMA	−0.1548	0.3273	2.14	.049*
PMd → PMv	0.2505	0.5050	2.00	.055
PMv → PMd	−0.2672	0.9784	2.37	.034*
Modulation				
Word repetition	−0.1182	0.3567	1.65	.110
Pseudoword repetition	0.4317	0.4598	6.42	<.0001**
Driving Input				
Pre-SMA	0.4502	0.3954	7.34	<.0001**

*Significant at $p < .05$, two-tailed.

**Survives a Bonferroni correction for multiple comparisons ($p < .0055$).

Probabilistic Fiber Tracking Approach

Fibers connecting our fMRI-based seed regions in the pre-SMA, and the left PMd or pre-SMA and PMv were identified by multiplying the one-sided probability maps derived from the respective seed regions. Our results show a direct connection between pre-SMA and PMd as well as pre-SMA and PMv, presumably via direct local neighboring association fibers (Schmahmann, Smith, Eichler, & Filley, 2008; Figure 6).

DISCUSSION

Here we used DCM to investigate task-related influences between premotor areas during overt pseudoword repetition. We first identified three key regions that showed increased fMRI activation during modality-independent repetition of pseudowords and words: the bilateral pre-SMA, left PMd, and left PMv. These areas have been previously implicated in pseudoword repetition, reading, or production (Peeva et al., 2010; Saur et al., 2008; Mechelli et al., 2005). We then used DCM to identify the direction of influences exerted within this network. Our connectivity analyses extend previous neuroimaging studies on speech repetition in three ways.

First, the optimal DCM identified the pre-SMA as the most likely source of the driving input within the premotor network for pseudoword repetition. In our model space, each model of interregional connections was crossed with seven possible ways of the stimuli to enter our premotor network. This enabled us to test where the speech stimuli most likely entered our system. Our results provided strong evidence (i.e., an exceedance probability of 81% relative to 11% for the second best model) in favor of the pre-SMA relative to PMd and PMv and all possible combinations among these regions. This was supported by a family analysis that identified the family of models with driving input to pre-SMA as winning family of the seven families tested with an exceedance probability of 86%.

Second, our model provides direct evidence for an increased functional influence of bilateral pre-SMA on left PMd during the repetition of pseudowords. This was indicated by the strong task-specific increase in effective connectivity from pre-SMA to left PMd during the repetition of pseudowords whereas previous studies only demonstrated coactivation of these areas during fMRI. In this context, we wish to emphasize that DCM provides information about the direction of the interregional connections rather than implying nondirectional correlations (Friston et al., 2003). Of note, the task-related influence of pre-SMA on PMd in our winning model was modulated significantly more strongly by pseudoword repetition than word repetition.

Third, task-related influence from pre-SMA to PMd was facilitatory rather than inhibitory as indicated by the positive mean parameter estimates in the winning model. The

modulatory influence of pseudoword repetition on this connection in our winning model corresponded to an increase in facilitatory connectivity of more than 100% relative to the intrinsic connection strength. On the basis of the results from previous fMRI studies, a suppressive influence of pre-SMA on PMd activity might have been expected. For instance, activation of the pre-SMA has been reported during the successful inhibition of speech and motor hand responses in a stop-signal paradigm when participants were asked to inhibit their responses (i.e., naming of letters or pseudowords and button presses; Xue et al., 2008). A contribution of the pre-SMA to motor inhibition was also found in previous studies using stop-signal paradigms (Aron & Poldrack, 2006). Accordingly, one might argue that the increased pre-SMA activation during pseudoword repetition in our study reflected the inhibition of more prepotent familiar responses (i.e., words that are similar but different to the stimulus). If this were the case, then the pre-SMA should have an inhibitory influence on lateral premotor areas. However, context-dependent modulation of connections between pre-SMA and PMd during pseudoword repetition was rather facilitatory. We would argue that our task minimized the demands on inhibition, competitive responses, or rapid task switching because pseudowords and words were presented in blocks of six items of the same type. Although our results do not preclude a role of the pre-SMA in response inhibition, they suggest a significant facilitatory interaction from pre-SMA to PMd in the context of pseudoword repetition.

We did not find evidence that pseudoword repetition increased the influence of the pre-SMA on the more PMv region. Interestingly, there were trends in our winning model toward an inhibitory intrinsic connection between PMv and PMd as well as PMv and pre-SMA in the absence of any modulating experimental effects of pseudoword repetition. Although this does not preclude a role of the PMv in speech repetition, we suggest that the repetition of pseudowords primarily requires a close facilitatory interaction from pre-SMA to PMd.

Together, these findings suggest a supervisory role of the pre-SMA on PMd during pseudoword repetition. This fits with previous observations of increased coactivation of pre-SMA and PMd during motor response selection (Sakai et al., 2000). It also fits with previous suggestions that the pre-SMA initiates speech production (Ackermann & Ziegler, 2010) and plays a key role in the control of sequential movements (Tanji & Hoshi, 2001; Halsband et al., 1993) by coordinating the serial position or timing of syllable production (Bohland & Guenther, 2006). The increased facilitatory influence of the pre-SMA on PMd that we observed for pseudoword relative to word repetition can therefore be attributed to the increased load on the sequencing of motor plans when novel combinations of syllables need to be articulated.

With respect to the precise role of the premotor regions in speech, we found that, although the direct comparison of pseudoword to word repetition significantly increased pre-SMA activation (irrespective of modality), pseudowords had a relatively weak effect on the lateral premotor areas. Moreover, we found a stronger influence of pseudoword repetition on the connection from pre-SMA to PMd than from pre-SMA to PMv. These results highlight the different roles for our three premotor areas. Previous studies have reported increased activity in left PMd during motor speech preparation and execution (Mechelli et al., 2005; Paulesu et al., 2003; Salmelin, Schnitzler, Schmitz, & Freund, 2000) consistent with a role in the conversion of an abstract planned sequence into an effective motor plan during overt articulation (Alario et al., 2006). On the basis of previous studies, we therefore propose that the sequencing of complex unfamiliar pseudoword stimuli enhances the interaction between pre-SMA and PMd, with PMd involved in converting abstract planned sequences into an effective motor plan (Alario et al., 2006) and PMv involved in representing the anticipated speech sounds that are associated with the articulation of familiar phonemes or syllables (Guenther et al., 2006).

Goldberg (1985) suggested two different networks for motor control of language output based on the response mode with an activity shift from (pre-)SMA to lateral premotor areas from internally to externally specified actions. Whereas a stronger involvement of the pre-SMA in internally cued language tasks was supported by the results of more recent imaging studies (Tremblay & Gracco, 2006, 2010; Alario et al., 2006; Crosson et al., 2001), some studies provided evidence for a participation of lateral premotor areas in both internally and externally specified speech (Tremblay & Small, 2011; Tremblay & Gracco, 2006, 2010).

Nevertheless, a stronger activation for higher-order volitional production tasks compared with more externally constrained tasks, such as repetition, does not mean that the pre-SMA is exclusively contributing to internally specified tasks. Indeed, our results provide strong evidence for a key role of the pre-SMA in pseudoword repetition, which is in line with numerous other studies reporting pre-SMA activation during externally specified tasks like syllable or phoneme repetition (Peeva et al., 2010; Papoutsi et al., 2009; Rauschecker et al., 2008; Burton et al., 2001). Our finding of increased effective connectivity from pre-SMA to PMd during pseudoword repetition would therefore be compatible with the notion of overlapping rather than exclusionary roles for both regions in externally and internally guided movements (Tremblay & Gracco, 2006; Passingham, 1993).

The above-cited studies suggest that the pre-SMA is engaged in different processes during language production, that is, response selection and motor preparation of stimuli with increased sequencing difficulty. We believe that these findings are not contradictory as both functions occur at different stages of the production process and the pre-SMA appears to be a multimodal area engaged in different motor tasks and effector domains (Tremblay &

Gracco, 2010). The results of Braun, Guillemin, Hosey, and Varga (2001) also provide evidence for a key contribution of the pre-SMA to both the selection of speech movements and articulatory planning. In their study, the pre-SMA was activated during both the sequencing of complex internally guided speech movements and tasks that required complex praxic demands. Because the latter did not necessarily require the encoding of semantic information, it was argued that this area plays a key role in the later stages of language production, that is, the phonological encoding and organization of coordinated muscular activity related to articulation (Braun et al., 2001).

Finally, we found direct anatomical connections between pre-SMA and both PMd as well as PMv. Whereas previous studies in humans have not investigated anatomical connections between pre-SMA and PMd or PMv, our results are supported by a large body of animal studies. Accordingly, previous in vivo tracer studies in monkeys reported dense connections between the homologue of human pre-SMA (Area F6) and both the homologues of human PMd (Areas F2/F7) and PMv (Area F4/F5; Gerbella, Belmalih, Borra, Rozzi, & Luppino, 2011; Liu, Morel, Wannier, & Rouiller, 2002; Luppino & Rizzolatti, 2000). This shows that, although the pre-SMA is structurally connected with both lateral premotor areas, these regions differ with respect to their functional connectivity profiles with pre-SMA showing an increased task-related influence on PMd but not PMv during pseudoword repetition.

With respect to the problem of movement-induced artifacts induced by overt speech, it should be noted that, although some studies used covert language production paradigms to avoid motion induced artifacts from overt articulation (Rauschecker et al., 2008; Wildgruber, Ackermann, & Grodd, 2001), it has been demonstrated that activations during overt speech differ in some aspects from covert speech (Shuster & Lemieux, 2005; Riecker et al., 2000). We used the unwarping tool provided in the SPM software to correct for motion-induced artifacts during overt stimulus repetition. Because our speech stimuli had an average duration of well below 2 sec, we would argue that it should be possible to temporally dissociate motion artifacts and the BOLD signal for the verbal output (Haller, Radue, Erb, Grodd, & Kircher, 2005). In summary, we are confident that our results were not confounded by movement-induced artifacts.

Acknowledgments

The experiments conducted at the Department of Neurology, Christian-Albrechts-University, in Kiel, were funded by the Bundesministerium für Bildung und Forschung (Grant 01GW0663). G. H. was supported by the Deutsche Forschungsgemeinschaft (DFG; HA 6314/1-1). H. R. S. was supported by the Bundesministerium für Bildung und Forschung (01GO0511 "NeuroImageNord") and a grant of excellence sponsored by The Lundbeck Foundation Mapping, Modulation and Modeling the Control of Actions (ContAct) (R59 A5399).

Reprint requests should be sent to Gesa Hartwigsen, Language and Aphasia Laboratory, Department of Neurology, University of Leipzig, Liebigstrasse 20, 04103 Leipzig, Germany, or via e-mail: gesa.hartwigsen@medizin.uni-leipzig.de.

REFERENCES

Ackermann, H., & Ziegler, W. (2010). Brain mechanisms underlying speech motor control. In W. J. Hardcastle, J. Laver, & F. E. Gibbons (Eds.), *The handbook of phonetic sciences* (Vol. 2, pp. 202–250). Malden, MA: Wiley-Blackwell.

Alario, F. X., Chainay, H., Lehericy, S., & Cohen, L. (2006). The role of the supplementary motor area (SMA) in word production. *Brain Research, 1076,* 129–143.

Alm, P. A. (2004). Stuttering and the basal ganglia circuits: A critical review of possible relations. *Journal of Communication Disorders, 37,* 325–369.

Andersson, J. L., Hutton, C., Ashburner, J., Turner, R., & Friston, K. (2001). Modeling geometric deformations in EPI time series. *Neuroimage, 13,* 903–919.

Aron, A. R., & Poldrack, R. A. (2006). Cortical and subcortical contributions to stop signal response inhibition: Role of the subthalamic nucleus. *Journal of Neuroscience, 26,* 2424–2433.

Basser, P. J., Mattiello, J., & LeBihan, D. (1994). Estimation of the effective self-diffusion tensor from the NMR spin echo. *Journal of Magnetic Resonance, Series B, 103,* 247–254.

Bohland, J. W., & Guenther, F. H. (2006). An fMRI investigation of syllable sequence production. *Neuroimage, 32,* 821–841.

Botez, M. I., & Barbeau, A. (1971). Role of subcortical structures, and particularly of the thalamus, in the mechanisms of speech and language. A review. *International Journal of Neurology, 8,* 300–320.

Braun, A. R., Guillemin, A., Hosey, L., & Varga, M. (2001). The neural organization of discourse: An H2 15O-PET study of narrative production in English and American sign language. *Brain, 124,* 2028–2044.

Burton, M. W., Noll, D. C., & Small, S. L. (2001). The anatomy of auditory word processing: Individual variability. *Brain and Language, 77,* 119–131.

Crosson, B., Sadek, J. R., Maron, L., Gokcay, D., Mohr, C., Auerbach, E. J., et al. (2001). Relative shift in activity from medial to lateral frontal cortex during internally versus externally guided word generation. *Journal of Cognitive Neuroscience, 13,* 272–283.

den Ouden, D. B., Saur, D., Mader, W., Schelter, B., Lukic, S., Wali, E., et al. (2012). Network modulation during complex syntactic processing. *Neuroimage, 59,* 815–823.

Devlin, J. T., Matthews, P. M., & Rushworth, M. F. (2003). Semantic processing in the left inferior prefrontal cortex: A combined functional magnetic resonance imaging and transcranial magnetic stimulation study. *Journal of Cognitive Neuroscience, 15,* 71–84.

Dollaghan, C., & Campbell, T. F. (1998). Nonword repetition and child language impairment. *Journal of Speech, Language, and Hearing Research, 41,* 1136–1146.

Duyck, W., Desmet, T., Verbeke, L. P., & Brysbaert, M. (2004). WordGen: A tool for word selection and nonword generation in Dutch, English, German, and French. *Behavior Research Methods, Instruments, & Computers, 36,* 488–499.

Eickhoff, S. B., Stephan, K. E., Mohlberg, H., Grefkes, C., Fink, G. R., Amunts, K., et al. (2005). A new SPM toolbox for combining probabilistic cytoarchitectonic maps and functional imaging data. *Neuroimage, 25,* 1325–1335.

Friston, K. J., Ashburner, J., Frith, C. D., Poline, J.-B., Heather, J. D., & Frackowiak, R. S. J. (1995). Spatial registration and normalization of images. *Human Brain Mapping, 3,* 165–189.

Friston, K. J., Buechel, C., Fink, G. R., Morris, J., Rolls, E., & Dolan, R. J. (1997). Psychophysiological and modulatory interactions in neuroimaging. *Neuroimage, 6,* 218–229.

Friston, K. J., Harrison, L., & Penny, W. (2003). Dynamic causal modelling. *Neuroimage, 19,* 1273–1302.

Friston, K. J., Holmes, A. P., Worsley, K. J., Poline, J.-B., Frith, C. D., & Frackowiak, R. S. J. (1995). Statistical parametric maps in functional imaging: A general linear approach. *Human Brain Mapping, 2,* 189–210.

Friston, K. J., Stephan, K. E., Lund, T. E., Morcom, A., & Kiebel, S. (2005). Mixed-effects and fMRI studies. *Neuroimage, 24,* 244–252.

Gerbella, M., Belmalih, A., Borra, E., Rozzi, S., & Luppino, G. (2011). Cortical connections of the anterior (F5a) subdivision of the macaque ventral premotor area F5. *Brain Structure and Function, 216,* 43–65.

Goldberg, G. (1985). Supplementary motor area structure and function: Review and hypotheses. *Behavioral and Brain Sciences, 8,* 567–616.

Guenther, F. H., Ghosh, S. S., & Tourville, J. A. (2006). Neural modeling and imaging of the cortical interactions underlying syllable production. *Brain and Language, 96,* 280–301.

Haller, S., Radue, E. W., Erb, M., Grodd, W., & Kircher, T. (2005). Overt sentence production in event-related fMRI. *Neuropsychologia, 43,* 807–814.

Halsband, U., Ito, N., Tanji, J., & Freund, H. J. (1993). The role of premotor cortex and the supplementary motor area in the temporal control of movement in man. *Brain, 116,* 243–266.

Hartwigsen, G., Baumgaertner, A., Price, C. J., Koehnke, M., Ulmer, S., & Siebner, H. R. (2010). Efficient phonological decisions require both the left and right supramarginal gyri. *Proceedings of the National Academy of Sciences, U.S.A., 107,* 16494–16499.

Hickok, G., Houde, J., & Rong, F. (2011). Sensorimotor integration in speech processing: Computational basis and neural organization. *Neuron, 69,* 407–422.

Hickok, G., & Poeppel, D. (2004). Dorsal and ventral streams: A framework for understanding aspects of the functional anatomy of language. *Cognition, 92,* 67–99.

Kreher, B. W., Schnell, S., Mader, I., Il'yasov, K. A., Hennig, J., Kiselev, V. G., et al. (2008). Connecting and merging fibres: Pathway extraction by combining probability maps. *Neuroimage, 43,* 81–89.

Leff, A. P., Schofield, T. M., Stephan, K. E., Crinion, J. T., Friston, K. J., & Price, C. J. (2008). The cortical dynamics of intelligible speech. *Journal of Neuroscience, 28,* 13209–13215.

Liu, J., Morel, A., Wannier, T., Rouillier, E. M. (2002). Origins of callosal projections to the supplementary motor area (SMA): A direct comparison between pre-SMA and SMA-proper in macaque monkeys. *Journal of Comparative Neurology, 443,* 71–85.

Luppino, G., & Rizzolatti, G. (2000). The organization of the frontal motor cortex. *News in Physiological Sciences, 15,* 219–224.

Mayka, M. A., Corcos, D. M., Leurgans, S. E., & Vaillancourt, D. E. (2006). Three-dimensional locations and boundaries of motor and premotor cortices as defined by functional brain imaging: A meta-analysis. *Neuroimage, 31,* 1453–1474.

Mechelli, A., Crinion, J. T., Long, S., Friston, K. J., Lambon Ralph, M. A., Patterson, K., et al. (2005). Dissociating reading processes on the basis of neuronal interactions. *Journal of Cognitive Neuroscience, 17,* 1753–1765.

Nichols, T., Brett, M., Andersson, J., Wager, T., & Poline, J. B. (2005). Valid conjunction inference with the minimum statistic. *Neuroimage, 25,* 653–660.

Oldfield, R. C. (1971). The assessment and analysis of handedness: The Edinburgh inventory. *Neuropsychologia, 9,* 97–113.

Papoutsi, M., de Zwart, J. A., Jansma, J. M., Pickering, M. J., Bednar, J. A., & Horwitz, B. (2009). From phonemes to articulatory codes: An fMRI study of the role of Broca's area in speech production. *Cerebral Cortex, 19,* 2156–2165.

Passingham, R. E. (1993). *The frontal lobes and voluntary action*. New York: Oxford University Press.

Paulesu, E., Perani, D., Blasi, V., Silani, G., Borghese, N. A., De Giovanni, U., et al. (2003). A functional-anatomical model for lipreading. *Journal of Neurophysiology, 90,* 2005–2013.

Peeva, M. G., Guenther, F. H., Tourville, J. A., Nieto-Castanon, A., Anton, J. L., Nazarian, B., et al. (2010). Distinct representations of phonemes, syllables, and supra-syllabic sequences in the speech production network. *Neuroimage, 50,* 626–638.

Price, C. J. (2000). The anatomy of language: Contributions from functional neuroimaging. *Journal of Anatomy, 197,* 335–359.

Rauschecker, A. M., Pringle, A., & Watkins, K. E. (2008). Changes in neural activity associated with learning to articulate novel auditory pseudowords by covert repetition. *Human Brain Mapping, 29,* 1231–1242.

Richardson, F. M., Seghier, M. L., Leff, A. P., Thomas, M. S., & Price, C. J. (2011). Multiple routes from occipital to temporal cortices during reading. *Journal of Neuroscience, 31,* 8239–8247.

Riecker, A., Ackermann, H., Wildgruber, D., Meyer, J., Dogil, G., Haider, H., et al. (2000). Articulatory/phonetic sequencing at the level of the anterior perisylvian cortex: A functional magnetic resonance imaging (fMRI) study. *Brain and Language, 75,* 259–276.

Sakai, K., Hikosaka, O., Takino, R., Miyauchi, S., Nielsen, M., & Tamada, T. (2000). What and when: Parallel and convergent processing in motor control. *Journal of Neuroscience, 20,* 2691–2700.

Salmelin, R., Schnitzler, A., Schmitz, F., & Freund, H. (2000). Single word reading in developmental stutterers and fluent speakers. *Brain, 123,* 1184–1202.

Saur, D., Kreher, B. W., Schnell, S., Kummerer, D., Kellmeyer, P., Vry, M. S., et al. (2008). Ventral and dorsal pathways for language. *Proceedings of the National Academy of Sciences, U.S.A., 105,* 18035–18040.

Schmahmann, J. D., Smith, E. E., Eichler, F. S., & Filley, C. M. (2008). Cerebral white matter: Neuroanatomy, clinical neurology, and neurobehavioral correlates. *Annals of the New York Academy of Sciences, 1142,* 266–309.

Seghier, M. L., Josse, G., Leff, A. P., & Price, C. J. (2011). Lateralization is predicted by reduced coupling from the left to right prefrontal cortex during semantic decisions on written words. *Cerebral Cortex, 21,* 1519–1531.

Shima, K., & Tanji, J. (2000). Neuronal activity in the supplementary and presupplementary motor areas for temporal organization of multiple movements. *Journal of Neurophysiology, 84,* 2148–2160.

Shuster, L. I., & Lemieux, S. K. (2005). An fMRI investigation of covertly and overtly produced mono- and multisyllabic words. *Brain and Language, 93,* 20–31.

Sörös, P., Sokoloff, L. G., Bose, A., McIntosh, A. R., Graham, S. J., & Stuss, D. T. (2006). Clustered functional MRI of overt speech production. *Neuroimage, 32,* 376–387.

Stephan, K. E., Penny, W. D., Moran, R. J., den Ouden, H. E., Daunizeau, J., & Friston, K. J. (2010). Ten simple rules for dynamic causal modeling. *Neuroimage, 49,* 3099–3109.

Tanji, J., & Hoshi, E. (2001). Behavioral planning in the prefrontal cortex. *Current Opinion in Neurobiology, 11,* 164–170.
Tremblay, P., & Gracco, V. L. (2006). Contribution of the frontal lobe to externally and internally specified verbal responses: fMRI evidence. *Neuroimage, 33,* 947–957.
Tremblay, P., & Gracco, V. L. (2010). On the selection of words and oral motor responses: Evidence of a response-independent frontoparietal network. *Cortex, 46,* 15–28.
Tremblay, P., & Small, S. L. (2011). Motor response selection in overt sentence production: A functional MRI study. *Frontiers in Psychology, 2,* 253.
Wildgruber, D., Ackermann, H., & Grodd, W. (2001). Differential contributions of motor cortex, basal ganglia, and cerebellum to speech motor control: Effects of syllable repetition rate evaluated by fMRI. *Neuroimage, 13,* 101–109.
Xue, G., Aron, A. R., & Poldrack, R. A. (2008). Common neural substrates for inhibition of spoken and manual responses. *Cerebral Cortex, 18,* 1923–1932.
Ziegler, W., Kilian, B., & Deger, K. (1997). The role of the left mesial frontal cortex in fluent speech: Evidence from a case of left supplementary motor area hemorrhage. *Neuropsychologia, 35,* 1197–1208.